Article

Ligand Effects on the Ferro- to Antiferromagnetic Exchange Ratio in Bis(*o*-Semiquinonato)copper(II)

Victor I. Ovcharenko, Elena V. Gorelik, Sergey V. Fokin, Galina V. Romanenko,
Vladimir N. Ikorskii, Anna V. Krashilina, Vladimir K. Cherkasov, and Gleb A. Abakumov

J. Am. Chem. Soc., **2007**, 129 (34), 10512-10521• DOI: 10.1021/ja072463b • Publication Date (Web): 03 August 2007

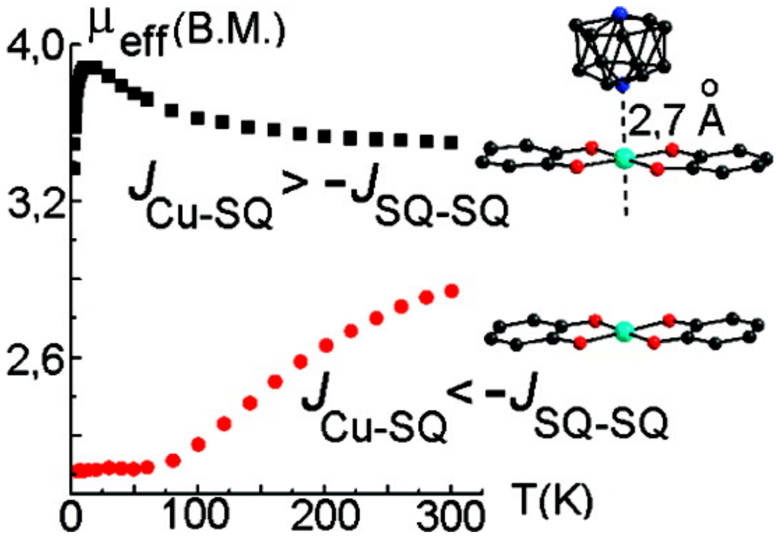

Journal of the American Chemical Society is published by the American Chemical Society. 1155 Sixteenth Street N.W., Washington, DC 20036

J|A|C|S
ARTICLES
Published on Web 08/03/2007

Ligand Effects on the Ferro- to Antiferromagnetic Exchange Ratio in Bis(*o*-Semiquinonato)copper(II)

Victor I. Ovcharenko,*,† Elena V. Gorelik,† Sergey V. Fokin,† Galina V. Romanenko,†
Vladimir N. Ikorskii,† Anna V. Krashilina,‡ Vladimir K. Cherkasov,*,‡ and
Gleb A. Abakumov‡

Contribution from the International Tomography Center, Russian Academy of Sciences,
3A Institutskaya Street, 630090 Novosibirsk, Russian Federation, and G. A. Razuvaev Institute
of Organometallic Chemistry, Russian Academy of Sciences, 49 Tropinina Street,
603600 Nizhny Novgorod, Russian Federation

Received April 9, 2007; E-mail: Victor.Ovcharenko@tomo.nsc.ru; cherkasov@iomc.ras.ru

Abstract: Heterospin complexes $[Cu(SQ)_2Py]\cdot C_7H_8$, $Cu(SQ)_2DABCO$, and $[Cu(SQ)_2NIT\text{-}m Py]\cdot C_6H_6$, where $Cu(SQ)_2$ is bis(3,6-di-*tert*-butyl-*o*-benzosemiquinonato)copper(II), DABCO is 1,4-diazabicyclo(2,2,2)octane, and NIT-*m*Py is the nitronyl nitroxide 2-(pyridin-3-yl)-4,4,5,5-tetramethyl-4,5-dihydro-1*H*-imidazole-3-oxide-1-oxyl, have been synthesized. The molecules of these complexes have a specific combination of the intramolecular ferro- and antiferromagnetic exchange interactions between the odd electrons of Cu(II) and SQ ligands, characterized by large exchange coupling parameters $|J| \approx 100-300$ cm^{-1}. X-ray and magnetochemical studies of a series of mixed-ligand compounds revealed that an extra ligand (Py, NIT-*m*Py, or DABCO) coordinated to the metal atom produces a dramatic effect on the magnetic properties of the complex, changing the multiplicity of the ground state. Quantum chemical analysis of magnetostructural correlations showed that the energy of the antiferromagnetic exchange interaction between the odd electrons of the SQ ligands in the $Cu(SQ)_2$ bischelate is extremely sensitive to both the nature of the extra ligand and structural distortions of the coordination unit, arising from extra ligand coordination.

Introduction

Transition metal complexes with *o*-semiquinonate ligands, characterized by valence tautomerism,[1] are valuable objects for molecular spintronics.[2] Systematic investigations of the specific photoinduced and thermally induced magnetic effects inherent in compounds from this class show great promise for creating components of sensors and switches that are sensitive to external effects.[3] Photo(thermo)activation of metal *o*-semiquinonates is occasionally accompanied by pronounced deformation of crystals. Thus, needle-like crystals of rhodium and cobalt *o*-semiquinonates are reversibly bent by photo(thermo)activation (bending crystals) but revert to their initial state after deactivation.[4] These effects suggest that metal semiquinonates possess stereochemical nonrigidity at a molecular level.

We are interested in bis(3,6-di-*tert*-butyl-*o*-benzosemiquinonato)copper(II) $[Cu(SQ)_2]$ as a stereochemically nonrigid metal-containing matrix for the following reasons: Recently, "breathing crystals" of stereochemically nonrigid heterospin complexes of bis(hexafluoroacetylacetonato)copper(II) and nitronyl nitroxides have been found, which are also capable of being reversibly deformed during repeated cooling−heating cycles.[5] Previously, there were no publications on mixed-ligand

---

† International Tomography Center, Novosibirsk.

‡ Institute of Organometallic Chemistry, Nizhny Novgorod.

(1) (a) Buchanan, R. M.; Pierpont, C. G. *J. Am. Chem. Soc*. **1980**, *102*, 4951−4957. (b) Jung, O.-S.; Pierpont, C. G. *Inorg. Chem*. **1994**, *33*, 2227−2235. (c) Attia, S. A.; Jung, O.-S.; Pierpont, C. G. *Inorg. Chim. Acta* **1994**, *226*, 91−98. (d) Attia, S. A.; Bhattacharya, S.; Pierpont, C. G. *Inorg. Chem*. **1995**, *34*, 4427−4433. (e) Attia, S. A.; Pierpont, C. G. *Inorg. Chem*. **1995**, *34*, 1172−1179. (f) Pierpont, C. G.; Lange, C. W. *Prog. Inorg. Chem*. **1994**, *41*, 331−442. (g) Pierpont, C. G. *Coord. Chem. Rev*. **2001**, *216−217*, 99−125. (h) Ohtsu, H.; Tanaka, K. *Angew. Chem., Int. Ed*. **2004**, *43*, 6301−6303. (i) Abakumov, G. A.; Razuvaev, G. A.; Nevodchikov, V. I.; Cherkasov, V. K. *J. Organomet. Chem*. **1988**, *341*, 485−494. (j) Abakumov, G. A.; Garnov, V. A.; Nevodchikov, V. I.; Cherkasov, V. K. *Dokl. Akad. Nauk SSSR* **1989**, *304*, 107−109.

(2) (a) Shultz, D. A.; Sloop, J. C.; Washington, G. *J. Org. Chem*. **2006**, *71*, 9104−9113. (b) Shultz, D. A. In *Magnetism: Molecules to Materials, II: Molecular-Based Materials*; Miller, J. S., Drillon, M., Eds.; Wiley-VCH: New York, 2001; pp 281−306. (c) Hendrickson, D. N.; Pierpont, C. G. In *Topics in Current Chemistry*; Gütlich, P., Goodwin, H. A., Eds.; Springer-Verlag: Berlin, Heidelberg, 2004; Vol. 234, pp 64−95. (d) Gütlich, P.; Dei, A. *Angew. Chem., Int. Ed. Engl*. **1997**, *37*, 2734.

(3) (a) Jung, O.-S.; Jo, D. H.; Lee, Y.-A.; Conklin, B. J.; Pierpont, C. G. *Inorg. Chem*. **1997**, *36*, 19−24. (b) Caneschi, A.; Dei, A.; Fabrizi de Biani, F.; Gütlich, P.; Ksenofontov, V.; Levchenko, G.; Hoefer, A.; Renz, F. *Chem. Eur. J*. **2001**, *7*, 3926−3930. (c) Wolf, S. A.; Awschalom, D. D.; Buhrman, R. A.; Daughton, J. M.; von Molnar, S.; Roukes, M. L.; Chtchelkanova, A. Y.; Treger, D. M. *Science* **2001**, *294*, 1488−1495. (d) Moser, J.-E. *Nat. Mater*. **2005**, *4*, 723−724. (e) Tagami, K.; Tsukada, M. *J. Phys. Chem. B* **2004**, *108*, 6441−6444. (f) Yuasa, J.; Suenobu, T.; Fukuzumi, S. *J. Phys. Chem. A*. **2005**, *109*, 9356−9362. (g) Suenaga, Y.; Pierpont, C. G. *Inorg. Chem*. **2005**, *44*, 6183−6191. (h) Evangelio, E.; Ruiz-Molina, D. *Eur. J. Inorg. Chem*. **2005**, 2957−2971. (i) Sato, O. *J. Photochem. Photobiol. C: Photochem. Rev*. **2004**, *5*, 203−223. (j) Dei, A.; Gatteschi, D.; Sangregorio, C.; Sorace, L. *Acc. Chem. Res*. **2004**, *37*, 827−835. (k) Jung, O.-S.; Pierpont, C. G. *J. Am. Chem. Soc*. **1994**, *116*, 1127−1128. (l) Letard, J.-F.; Guionneau, P.; Goux-Capes, L. In *Topics in Current Chemistry*; Gütlich, P., Goodwin, H. A., Eds.; Springer-Verlag: Berlin, Heidelberg, 2004; Vol. 235, pp 221−249.

(4) (a) Abakumov, G. A.; Nevodchikov, V. I. *Dokl. Akad. Nauk SSSR* **1982**, *266*, 1407−1410. (b) Abakumov, G. A.; Cherkasov, V. K.; Bubnov, M. P.; Ellert, O. G.; Dobrokhotova, J. V.; Zakharov, L. N.; Struchkov, E. T. *Dokl. Chem*. **1993**, *328*, 12−14. (c) Lebedev, B. V.; Smirnova, N. N.; Abakumov, G. A.; Cherkasov, V. K.; Bubnov, M. P. *J. Chem. Thermodyn*. **2002**, *34*, 2093−2103. (d) Smirnova, N. N.; Abakumov, G. A.; Cherkasov, V. K.; Kozhanov, K. A.; Arapova, A. V.; Bubnov, M. P. *J. Chem. Thermodyn*. **2006**, *38*, 678−684.

10.1021/ja072463b CCC: $37.00

Chart 1

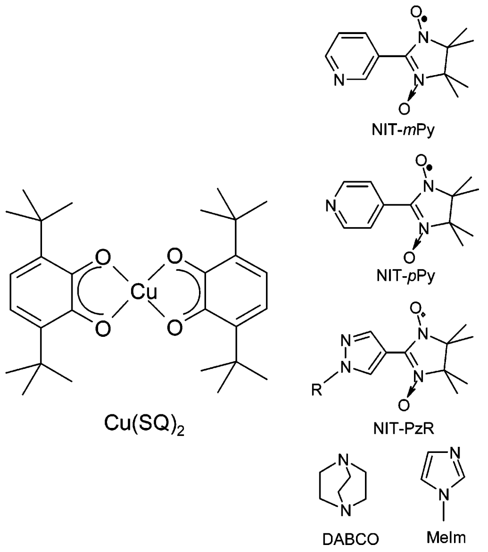

complexes containing the *o*-semiquinonato ligand along with nitronyl nitroxide (Chart 1) in their coordination sphere, although metal chelate complexes with *o*-semiquinonato and *o*-iminosemiquinonato ligands form a large, unique class of chemical compounds in which various heterospin exchange clusters are readily generated and have high spin coupling energies of paramagnetic centers.[6] The Cambridge Crystallographic Database contains no data about complexes of metal semiquinonates with nitroxides.[7] Shultz et al. reported on original metal semiquinonates in which the semiquinonato ligand contains a nitronyl nitroxide fragment as one of substituents.[8]

We succeeded in isolating a heterospin complex of Cu(SQ)$_2$ with nitronyl nitroxides NIT-*m*Py and studied its structure and magnetic properties. Analysis of magnetostructural correlations inherent in the complex revealed that intramolecular antiferromagnetic exchange interaction in Cu(SQ)$_2$ is suppressed by coordination of additional ligands. It became clear that this is a general effect, which is independent of whether the extra ligands are paramagnetic or diamagnetic.

Chart 2

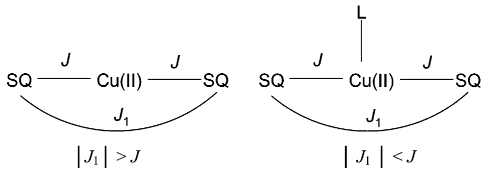

The exchange energy J_1 in the channel, i.e., the energy of exchange interaction between the odd electrons of the SQ ligands (Chart 2), turned out to be extremely sensitive to L in the coordination sphere of Cu(II). Quantum chemical analysis of exchange interactions confirmed that the parameter J_1 is highly sensitive to variation of the geometrical characteristics of the $\{SQ^{-\bullet}-Cu^{2+}-{}^{\bullet}SQ^{-}\}$ exchange cluster and to the extra ligand L incorporated in the coordination sphere of Cu(II).

Experimental Section

Sample Preparation. All the solvents used were reagent quality. 2,3-Bis(hydroxylamino)-2,3-dimethylbutane monosulfate monohydrate[9] and 2-(pyridin-3(4)-yl)-4,4,5,5-tetramethyl-4,5-dihydro-1*H*-imidazole-3-oxide-1-oxyl (NIT-*m*Py, NIT-*p*Py)[10] were synthesized according to known procedures. Bis(3,6-di-*tert*-butyl-*o*-benzosemiquinonato)copper(II) [Cu(SQ)$_2$] was synthesized by following procedure described elsewhere.[11] For X-ray analysis, Cu(SQ)$_2$ single crystals were grown from hexane.

[Cu(SQ)$_2$NIT-*m*Py]·C_6H_6. A solution of NIT-*m*Py (0.0500 g, 0.21 mmol) in benzene (2 mL) was added to a solution of Cu(SQ)$_2$ (0.1076 g, 0.21 mmol) in hexane (20 mL). The resulting solution was kept overnight at −18 °C. The dark green-brown crystalline precipitate suitable for an X-ray analysis was filtered off, washed with cold hexane, and dried in air. Yield 52%. Calculated for $C_{46}H_{62}N_3O6Cu$, %: C 67.7, H 7.7, N 5.2. Found, %: C 67.4, H 7.5, N 5.2. A similar procedure that used NIT-*p*Py instead of NIT-*m*Py led to the formation of black crystals of [Cu(SQ)$_2$NIT-*p*Py]·C_6H_6. Calculated for $C_{46}H_{62}N_3O_6Cu$, %: C 67.7, H 7.7, N 5.2. Found, %: C 67.3, H 7.8, N 5.1.

[Cu(SQ)$_2$Py]·C_7H_8. Pyridine (0.1 mL) was added to a solution of Cu(SQ)$_2$ (0.0500 g, 0.1 mmol) in toluene (5 mL). After the solution had been kept at −18 °C for 6 h, dark blue crystals suitable for an X-ray analysis precipitated. The crystals were filtered off, washed with cold toluene, and dried in air. Yield 32%. Calculated for $C_{40}H_{53}N_1O_4Cu$, %: C 71.1, H 7.9, N 2.1. Found, %: C 70.6, H 7.8, N 2.2. A similar procedure using diethyl ether instead of toluene formed dark blue crystals of [Cu(SQ)$_2$Py]·Et_2O, which were filtered off and washed with cold ether. The crystals quickly grew turbid in air. Yield 65%. Calculated for $C_{37}H_{55}NO_5Cu$, %: C 67.6, H 8.4, N 2.1. Found, %: C 67.0, H 8.1, N 2.2.

Cu(SQ)$_2$DABCO. A solution of 1,4-diazabicyclo(2.2.2)octane (0.07 g, 0.6 mmol) in toluene (10 mL) was added at 40 °C to a solution of Cu(SQ)$_2$ (0.200 g, 0.4 mmol) in toluene (15 mL). Dark blue needles formed immediately after thermostating of the reaction mixture had terminated. The crystals were filtered off, washed with toluene, and dried in air. This gave a quantitative yield. Calculated for $C_{34}H_{52}N_2O_4Cu$, %: C 66.3, H 8.5, Cu 10.3. Found, %: C 66.8, H 8.7, Cu 10.8.

---

(5) (a) Ovcharenko, V. I.; Fokin, S. V.; Romanenko, G. V.; Shvedenkov, Yu. G.; Ikorskii, V. N.; Tretyakov, E. V.; Vasilevsky, S. F. *Russ. J. Struct. Chem. (Engl. Transl.)* **2002**, *43*, 153−169. (b) Ovcharenko, V. I.; Maryunina, K. Yu.; Fokin, S. V.; Tretyakov, E. V.; Romanenko, G. V.; Ikorskii, V. N. *Russ. Chem. Bull. (Engl. Transl.)* **2004**, 2406−2427. (c) Ovcharenko, V. I.; Fokin, S. V.; Romanenko, G. V.; Ikorskii, V. N.; Tretyakov, E. V.; Vasilevsky, S. F.; Sagdeev, R. Z. *Mol. Phys.* **2002**, *100*, 1107−1115. (d) Rey, P.; Ovcharenko, V. I. In *Magnetism: Molecules to Materials, IV*; Miller, J. S., Drillon, M., Eds.; Wiley-VCH: New York, 2003; pp 41−63.

(6) (a) Pierpont, C. G.; Buchanan, R. M. *Coord. Chem. Rev.* **1981**, *38*, 45−86. (b) Pierpont, C. G. *Coord. Chem. Rev.* **2001**, *219*−*221*, 415−433. (c) Poddel'sky, A. I.; Cherkasov, V. K.; Bubnov, M. P.; Abakumova, L. G.; Abakumov, G. A. *J. Organomet. Chem.* **2005**, *690*, 145−150. (d) Chaudhuri, P.; Verani, C. N.; Bill, E.; Bothe, E.; Weyhermüller, T.; Wieghardt, K. *J. Am. Chem. Soc.* **2001**, *123*, 2213−2223. (e) Chun, H.; Verani, C. N.; Chaudhuri, P.; Bothe, E.; Bill, E.; Weyhermüller, T.; Wieghardt, K. *Inorg. Chem.* **2001**, *40*, 4157−4166. (f) Chun, H.; Chaudhuri, P.; Weyhermüller, T.; Wieghardt, K. *Inorg. Chem.* **2002**, *41*, 790−795. (g) Poddel'sky, A. I.; Cherkasov, V. K.; Fukin, G. K.; Bubnov, M. P.; Abakumova, L. G.; Abakumov, G. A. *Inorg. Chim. Acta* **2004**, *357*, 3632−3640. (h) Herebian, D.; Ghosh, P.; Chun, H.; Bothe, E.; Weyhermüller, T.; Wieghardt, K. *Eur. J. Inorg. Chem.* **2002**, 1957−1967. (i) Abakumov, G. A.; Cherkasov, V. K.; Poddel'sky, A. I.; Bubnov, M. P.; Abakumova, L. G.; Fukin, G. K. *Dokl. Chem. (Engl. Transl.)* **2004**, *399*, 207−210. (j) Bill, E.; Bothe, E.; Chaudhuri, P.; Chlopek, K.; Herebian, D.; Kokatam, S.; Ray, K.; Weyhermüller, T.; Neese, F.; Wieghardt, K. *Chem. Eur. J.* **2005**, *11*, 204−224. (k) Kahn, O.; Prins, R.; Reedijk, J.; Thompson, J. S. *Inorg. Chem*. **1987**, *26*, 3557−3561.

(7) Cambridge Structural Database, Version 5.28, 2007.

(8) (a) Shultz, D. A.; Bodnar, S. H.; Vostrikova, K. E.; Kampf, J. W. *Inorg. Chem*. **2000**, *39*, 6091−6093. (b) Shultz, D. A.; Vostrikova, K. E.; Bodnar, S. H.; Koo, H.-J.; Whangbo, M.-H.; Kirk, M. L.; Depperman, E. C.; Kampf, J. W. *J. Am. Chem. Soc*. **2003**, *125*, 1607−1617.

(9) (a) Ovcharenko, V.; Fokin, S.; Rey, P. *Mol. Cryst. Liq. Cryst.* **1999**, *334*, 109−119. (b) Ovcharenko, V. I.; Fokin, S. V.; Romanenko, G. V.; Korobkov, I. V.; Rey, P. *Russ. Chem. Bull. (Engl. Transl.)* **1999**, *48*, 1519−1525. (c) Hirel, C.; Vostrikova, K. E.; Pecaut, J.; Ovcharenko, V. I.; Rey, P. *Chem. Eur. J.* **2001**, *7*, 2007−2014.

(10) (a) Boocock, D. G. B.; Darcy, R.; Ullman, E. F. *J. Am. Chem. Soc.* **1968**, *90*, 5945−5946. (b) Ullman, E. F.; Osiecki, J. H.; Boocock, D. G. B.; Darcy, R. *J. Am. Chem. Soc*. **1972**, *94*, 7049−7059.

(11) Abakumov, G. A.; Cherkasov, V. K.; Bubnov, M. P.; Ellert, O. G.; Rakitin, Y. V.; Zakharov, L. N.; Struchkov, Y. T.; Safyanov, Y. N. *Russ. Chem. Bull.* **1992**, *41*, 1813−1818.

Table 1. Crystal Data and Selected Bond Distances (Å)

formula	$Cu(SQ)_2$	$Cu(SQ)_2$	$Cu(SQ)_2$-$PyEt_2O$	$Cu(SQ)_2$–PyC_7H_8	$[Cu(SQ)_2$-(NIT-*m*-Py)$]C_6H_6$	$Cu(SQ)_2$-DABCO	Cu(Cat)-$(Me_2Im)_2$
T, K	110	240	298	293	240	293	298
fw	504.14	504.14	637.20	674.37	816.53	616.32	896.11
crystal system	monoclinic	monoclinic	monoclinic	tetragonal	monoclinic	monoclinic	orthorhombic
space group	$P2_1/c$	$P2_1/c$	Pm	$P4_32_12$	$P2_1/c$	$C2$	$P2_12_12_1$
a, Å	9.763(5)	9.859(2)	10.3410(17)	10.3509(15)	22.851(3)	19.725(12)	7.1324(7)
b, Å	11.610(5)	11.654(3)	17.855(3)		11.908(2)	7.996(4)	17.6776(17)
c, Å	12.004(5)	12.090(3)	10.3418(17)	36.281(7)	17.448(3)	13.812(10)	18.2915(17)
β, deg	94.268(8)	94.391(5)	90.073(2)		108.990(3)	126.65(2)	
V, Å^3	1356.8(11)	1385.0(6)	1909.5(5)	3887.2(11)	4489.4(11)	1747.7(19)	2306.3(4)
Z	4	4	2	4	4	2	2
D_c, g·cm^{-3}	1.234	1.209	1.108	1.152	1.208	1.171	1.290
μ(Mo Kα), mm^{-1}	0.834	0.817	0.608	0.599	0.834	0.661	0.971
θ range, deg	2.44−23.30	2.07−23.29	1.14−23.30	1.12−23.27	1.88−23.31	1.84−23.49	2.23−23.33
I_{hkl} (meas/uniq)	5450/1911	4864/1929	14832/5700	16963/2801	17685/6442	6591/2538	17685/3323
R_{int}	0.0190	0.0372	0.0596	0.0568	0.0718	0.1222	0.0394
N	232	232	483	229	754	236	391
$R1^a$	0.0282	0.0358	0.0532	0.0749	0.0580	0.0654	0.0328
w$R2^a$ ($I > 2\sigma_I$)	0.0860	0.1018	0.1252	0.1697	0.1587	0.1258	0.0824
molecular site symmetry	C_i	C_i	C_s	C_2	C_1	C_2	C_1
Cu−O	1.908(1)	1.906(2)	1.932(4), 1.943(4)	1.942(3)	1.933(3), 1.944(3)	1.955(3)	1.891(2), 1.893(2)
	1.909(1)	1.913(2)	1.935(4), 1.934(4)	1.944(3)	1.948(3), 1.948(3)	1.957(3)	
Cu−N			2.296(8), 2.303(8)	2.305(7)	2.254(4)		1.998(2), 1.998(2)
C−O	1.287(2)	1.290(3)	1.275(6), 1.280(6)	1.280(5)	1.281(5), 1.289(5)	1.308(5)	1.339(3)
	1.288(2)	1.289(3)	1.278(7), 1.281(6)	1.280(5)	1.280(5), 1.278(5)	1.280(5)	1.336(3)
C1−C2	1.432(3)	1.430(3)	1.423(7), 1.444(7)	1.426(6)	1.430(6), 1.431(6)	1.422(6)	1.395(4)
	1.423(3)	1.429(3)	1.439(8), 1.428(7)	1.419(5)	1.437(6), 1.430(6)	1.453(6)	1.394(4)
C2−C4	1.362(3)	1.361(4)	1.351(7), 1.352(8)	1.341(6)	1.359(6), 1.369(6)	1.367(6)	1.385(4)
	1.361(3)	1.361(4)	1.345(7), 1.361(8)	1.335(6)	1.356(6), 1.350(6)	1.352(7)	1.388(4)
C4−C5	1.418(3)	1.420(4)	1.408(7), 1.397(7)	1.439(6)	1.420(7), 1.425(7)	1.429(7)	1.373(4)
C1−C8	1.463(3)	1.454(4)	1.456(6), 1.459(8)	1.486(5)	1.469(6), 1.470(6)	1.494(7)	1.427(4)
N−O					1.272(5), 1.286(4)		

[a] $R1 = \sum||F_o| - |F_c||/\sum|F_o|$; w$R2 = \{\sum[w(F_o^2 - F_c^2)^2]/\sum[w(F_o^2)^2]\}^{1/2}$; $w = 1/[\sigma^2(F_o^2) + (aP)^2 + bP]$ and $P = [2F_c^2 + F_o^2)]/3$.

$Cu(Cat)MeIm_2$. 1-Methylimidazole (0.1 mL) was added to a solution of $Cu(SQ)_2$ (0.0500 g, 0.1 mmol) in toluene (5 mL), and the mixture was allowed to stay overnight at −18°C. The resulting claret red crystals, suitable for an X-ray analysis, were filtered off, washed with cold hexane, and dried in air. Yield 47%. Anal. Calculated for $C_{22}H_{32}N_4O_2Cu$: C 59.0, H 7.2, N 12.5. Found, %: C 58.4, H 7.4, N 12.5.

Structure Analysis. For all compounds, diffraction reflections were collected on a Smart Apex (Bruker AXS) automatic diffractometer (λ Mo Kα, graphite monochromator) with an XY detector. The structures were solved by direct methods and refined by full-matrix least-squares fits (SHELX97 software). H atoms were located in difference syntheses of electron density and refined together with non-hydrogen atoms in an isotropic approximation. Crystal data, details of X-ray diffraction experiments, and selected bond distances for the complexes are given in Table 1. CIF files for the complexes can be found in the Supporting Information.

Magnetic Measurements. Magnetic measurements were carried out on an MPMS-5S SQUID magnetometer (Quantum Design) in the temperature range 2−300 K in a magnetic field of up to 45 kOe. Molar magnetic susceptibility χ was calculated using Pascal's additive scheme with corrections for diamagnetism of the compounds. The effective magnetic moment was calculated as $\mu_{eff} = (8\chi T)^{1/2}$. The program and scheme of calculations for heterospin clusters used for optimization in determining the exchange parameters of spin Hamiltonian are described elsewhere.[12]

DFT Calculations. All DFT calculations reported here were performed with the Gaussian 98 program package[13] using the B3LYP hybrid functional.[14] A precise all-electron Gaussian basis set of triple-ζ quality with one set of polarization functions, Wachters+f = (14s11p6d3f)/[8s6p4d1f][15] was employed for the copper atom as obtained from the Extensible Computational Chemistry Environment Basis Set Database.[16] All other atoms (e.g., C, N, and H) were described using the polarized 6-31G(d) basis set[17] of double-ζ quality. In all calculations, X-ray data for the complexes were used without further geometry optimization. In all cases, the $Cu(SQ)_2$DABCO chain complex was modeled by the individual $(CH_3)_3N-Cu(SQ)_2-N(CH_3)_3$ fragments. Molecular orbitals and spin density distributions were plotted with the Molekel program.[18]

---

[12] Ovcharenko, I. V.; Shvedenkov, Yu. G.; Musin, R. N.; Ikorskii, V. N. *J. Struct. Chem.* **1999**, *40*, 29−34.

[13] Frisch, M. J.; et al. *Gaussian 98*; Gaussian Inc.: Pittsburgh, PA, 1998.

[14] (a) Lee, C.; Yang, W.; Parr, R. G. *Phys. Rev. B* **1988**, *37*, 785−789. (b) Becke, A. D. *J. Chem. Phys.* **1993**, *98*, 5648−5652.

[15] (a) Wachters, A. J. H. *J. Chem. Phys.* **1970**, *52*, 1033−1036. (b) Wachters, A. J. H. IBM Technology Report RJ584, 1969. (c) Bauschlicher, C. W.; Langhoff, S. R., Jr.; Barnes, L. A. *J. Chem. Phys.* **1989**, *91*, 2399−2411.

Results and Discussion

Syntheses of Complexes. At the start of our investigation, we admitted the possibility that synthesis can form mixed-ligand complexes of Cu(SQ)$_2$ with nitronyl nitroxides containing a pyrazole or pyridine substituent in the side chain (Chart 1). Even the first experiments showed that, under the conditions of synthesis of Cu(hfac)$_2$NIT-PzR magnetoactive polymers,[5] bis(*o*-semiquinonato)copper(II), which has a substantially lower accepting ability than Cu(hfac)$_2$, did not react with pyrazolyl-substituted nitronyl nitroxides NIT-PzR. The crystals of the starting compounds were isolated as solids from the solutions containing mixtures of Cu(SQ)$_2$ and NIT-PzR, while reactions of Cu(SQ)$_2$ with pyridines NIT-*m*Py and NIT-*p*Py readily formed [Cu(SQ)$_2$NIT-*m*Py]·C_6H_6 and [Cu(SQ)$_2$NIT-*p*Py]·C_6H_6 heterospin complexes. However, the reaction mixture had to be cooled to about −15 to −20 °C because, at room temperature, storage of solutions of these complexes led to further transformations into unidentified products. Solutions of Cu(SQ)$_2$ containing a Py addition were more stable. In reactions of Cu(SQ)$_2$ with DABCO, the complex product was stable even after heating. The reaction of Cu(SQ)$_2$ with MeIm actually occurred during the stirring of reagents and was readily observed as a color change from blue to dark brown. A catecholate complex, Cu(Cat)MeIm$_2$, crystallized from these solutions. Thus, the kinetic stability of Cu(SQ)$_2$ in solution depended strongly on base additions to the reaction system.

Structure of Complexes. Structure analysis indicated that all compounds are molecular. Figure 1a−d shows a view of the molecules where the hydrogen atoms and the $(CH_3)_3C$ and CH_3 groups are omitted. In Figure 1a′−d′, these truncated molecules are shown in a special projection in which they may be viewed along the plane of the benzene rings. Combination of these projections clearly shows that the molecular fragments chosen are planar in solid Cu(SQ)$_2$ (Figure 1a,a′). The maximal deviation of atoms from the mean plane is up to 0.01 Å. All atoms of the coordination unit lie in this plane. The Cu−O distances are 1.907(2) and 1.913(2) Å, and the average C−O bond length is 1.289(3) Å. The structural parameters of the compound actually did not change (within the experimental error) after the temperature of the X-ray experiment was lowered from 240 to 110 K (Supporting Information). The structure of Cu(SQ)$_2$ was found to be similar to that of Ni(SQ)$_2$, as reported elsewhere,[11] although it was not investigated in detail previously. Note that the intermolecular distances between the paramagnetic centers are long enough. For example, the shortest distances between the copper atoms are 8.350 Å. This suggests that exchange interactions in solid Cu(SQ)$_2$, as well as in all other compounds being discussed, are mainly localized inside the chelate units of the individual molecules.

Without giving detailed structure description for other compounds, we report on only those structural features of the products that are relevant for further discussion. The most significant change in the structure of the coordination polyhedron on going from Cu(SQ)$_2$ to Py complexes is that pyridine “pulls” Cu out of the plane of O atoms of the semiquinonate ligands. The Cu atom deviates from this plane by 0.218(7) Å in [Cu(SQ)$_2$Py]·C_7H_8 and by 0.218(3) and 0.227(3) Å (two independent molecules) in [Cu(SQ)$_2$Py]·Et_2O (Figure 1b,b′). The Cu−N distances for the same molecules are 2.305(7), 2.296(8), and 2.303(8) Å, respectively. When the coordination number of Cu increases, the Cu−O distances in the coordination unit are elongated by 0.03−0.04 Å.

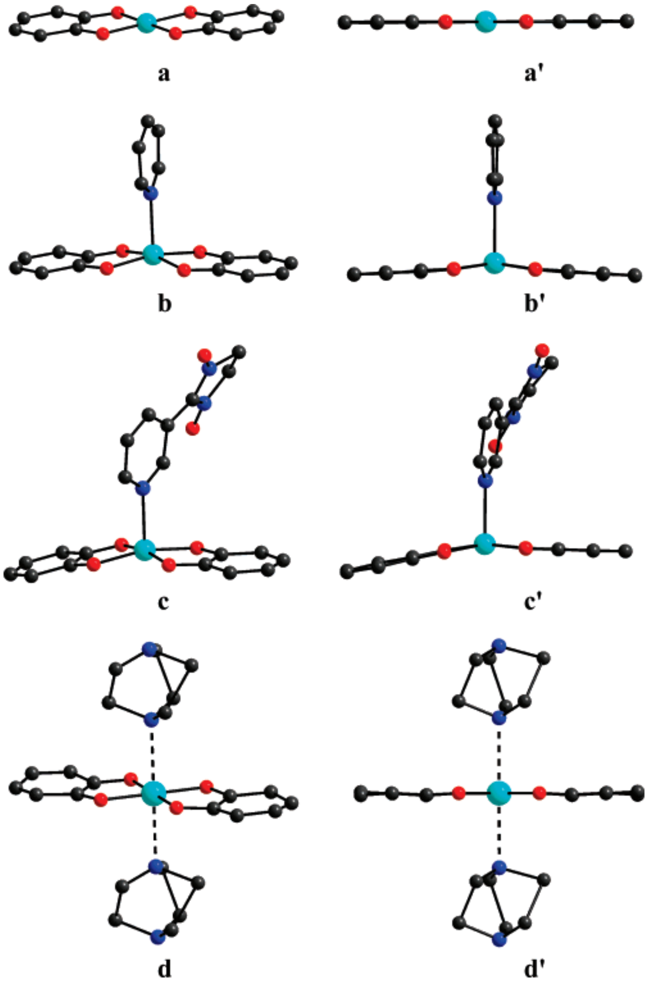

Figure 1. Two projections of the {Cu(SQ)$_2$} (a,a′), {Cu(SQ)$_2$Py} (b,b′), {Cu(SQ)$_2$NIT-*m*Py} (c,c′), and {DABCO-Cu(SQ)$_2$-DABCO} fragments (d,d′). Cu, sky blue ball; O, red ball; C, black ball; N, deep-blue ball. The $(CH_3)_3C$ groups of *o*-semiquinonates, the CH_3 groups of the imidazoline cycles, and the H atoms are omitted for clarity.

Figure 1c,c′ shows another mode of distortion of the $CuNO_4$ coordination unit formed in solid [Cu(SQ)$_2$NIT-*m*Py]·C_6H_6. In this case, the SQ ligands are essentially noncoplanar—one of them lies at an “angle” to the imaginary plane of the chelate unit. The Cu−O distances are similar to those in the Py complex; the Cu−N distance is reasonably short for the axially elongated Cu(II) complexes, 2.253(3) Å. In [Cu(SQ)$_2$NIT-*p*Py]·C_6H_6, the molecular fragment has a similar structure. However, in our experiments, single crystals of this complex were always imperfect and did not allow us to achieve an acceptable *R* index in X-ray experiments.

The DABCO solid complex consists of {Cu(SQ)$_2$DABCO}$_\infty$ polymer chains, in which copper lies in the same plane as the

---

(16) Basis sets were obtained from the Extensible Computational Chemistry Environment Basis Set Database, Version 02/02/06, as developed and distributed by the Molecular Science Computing Facility, Environmental and Molecular Sciences Laboratory, which is part of the Pacific Northwest Laboratory, P.O. Box 999, Richland, WA 99352, and funded by the U.S. Department of Energy. The Pacific Northwest Laboratory is a multi-program laboratory operated by Battelle Memorial Institute for the U.S. Department of Energy under contract DE-AC06-76RLO 1830. Contact Karen Schuchardt for further information.

(17) Davidson, E. R.; Feller, D. *Chem. Rev.* **1986**, *86*, 681−696.

(18) Portmann, S.; Lüthi, H. P. *CHIMIA* **2000**, *54*, 766−770.

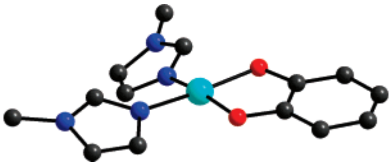

Figure 2. Molecular structure of Cu(Cat)MeIm$_2$. Cu, sky blue ball; O, red ball; N, deep-blue ball; C, black ball. The $(CH_3)_3C$ groups of catecholate and the H atoms are omitted for clarity.

Chart 3

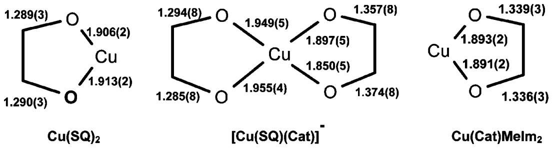

O atoms of the semiquinonate ligands (the deviation of the Cu atom from this plane is 0.003(8) Å) and the square environment of the Cu atom is completed to octahedral by the N atoms of the bridging DABCO molecules at Cu−N distances of 2.70(1) Å. In Figure 1d,d′, the recurrent fragment of the chain, {Cu(SQ)$_2$DABCO}, is completed by one more DABCO molecule in order to demonstrate the octahedral surroundings of the copper atom with an elongated N−Cu−N axis. The pronounced elongation of Cu−N distances in {Cu(SQ)$_2$DABCO}$_\infty$ relative to the values (∼2.4 Å) typical for axially elongated complexes of Cu(II), which is not observed in complexes with Py and NIT-*m*Py, is depicted in Figure 1d,d′ by the dashed lines for the bonds.

Thus, the results of our studies have actually confirmed that Cu(SQ)$_2$ is a stereochemically nonrigid matrix, the coordination unit of which can undergo various distortions depending on the spatial and electronic characteristics of the extra ligand.

As mentioned in the Sample Preparation section, interaction of Cu(SQ)$_2$ with MeIm led to decomposition of the starting bischelate, which formed crystals of the Cu(Cat)MeIm$_2$ catecholate complex (Figure 2). Chart 3 shows the Cu−O and O−C bond lengths in the chelate fragments of Cu(SQ)$_2$ and Cu(Cat)MeIm$_2$ and in the bis(1,4-di-*tert*-butyl-1,4-diazabuta-1,3-diene)copper(I) anion (3,6-di-*tert*-butyl-*o*-semiquinonato)(3,6-di-*tert*-butylcathecholato)copper(II) described previously.[19] It is clearly demonstrated that the semiquinonate and catecholate forms in the Cu complexes differ in the Cu−O and O−C bond lengths.[6a] In the case of the semiquinonate ligand, the Cu−O distances are >1.9 Å, and the C−O distances are <1.3 Å. For the catecholate ligand, the Cu−O bond in the metallocycle is shortened (<1.9 Å), while the C−O bond is lengthened (>1.3 Å).

Magnetic Properties. The temperature dependences of μ_{eff} differ substantially between the compounds. For Cu(SQ)$_2$, antiferromagnetic exchange interaction was clearly dominant (Figure 3). Theoretical analysis of exchange interactions within the exchange triad (Chart 2) using the spin Hamiltonian,

$$\hat{H} = -2J\,\hat{s}_{\text{Cu}}(\hat{s}_{\text{SQ1}} + \hat{s}_{\text{SQ2}}) - 2J_1\,\hat{s}_{\text{SQ1}}\,\hat{s}_{\text{SQ2}} - \beta[g_{\text{Cu}}\,\hat{s}_{\text{Cu}} + g_{\text{SQ}}(\hat{s}_{\text{SQ1}} + \hat{s}_{\text{SQ2}})]H - 2z\,J'\,\hat{S}\langle\hat{S}\rangle$$

gave $J = 136$ cm^{-1} and $J_1 = -203$ cm^{-1} ($g_{\text{Cu}} = 2.10$, $g_{\text{SQ}} = 2.0$). These values are close to the values (100 and −179 cm^{-1}) obtained by analyzing the dependences $\mu_{\text{eff}}(T)$ measured in a different temperature range (77−470 K), reported elsewhere.[11] They are also close to the values reported for square planar bis(*o*-iminobenzosemiquinonato)copper(II) complexes.[6d] The values of J and J_1 derived above are not claimed to be unique solutions, but they qualitatively demonstrate that spin coupling between the central Cu(II) ion and the terminal ligand radical is ferromagnetic and that coupling between two remote radical anions is highly antiferromagnetic. It was emphasized that superexchange energy is higher than direct exchange interaction energy ($|J_1| > J$). That is, in Cu(SQ)$_2$ molecules, the energy of the exchange interaction between the odd electrons of the semiquinonate ligands separated by long (SQ···SQ) distances is larger than the energy of exchange interaction between the paramagnetic centers lying at shorter SQ−Cu(II) distances. This is a nontrivial effect that demands (as stated elsewhere[11]) special quantum chemical investigations.

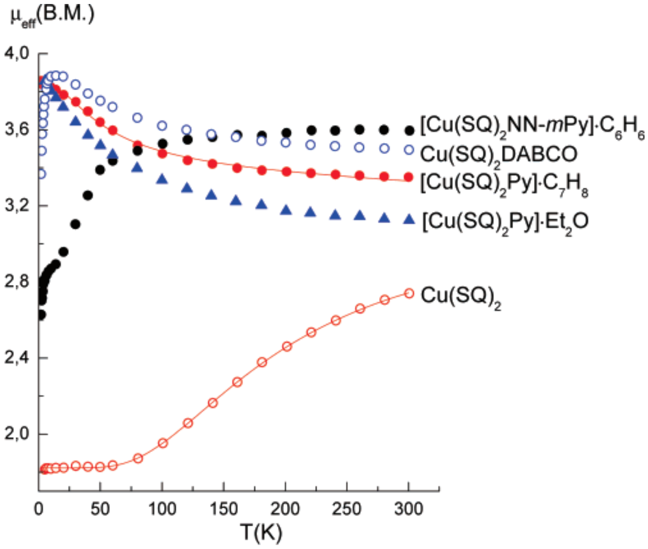

Figure 3. Temperature dependence of the effective magnetic moment of the complexes. Theoretical curves for Cu(SQ)$_2$ and [Cu(SQ)$_2$Py]·C_7H_8 (red solid lines).

However, nitroxyl radical coordination annihilated this effect in [Cu(SQ)$_2$NIT-*m*Py]·C_6H_6. Figure 3 shows that, in solid [Cu(SQ)$_2$NIT-*m*Py]·C_6H_6, ferro- and antiferromagnetic exchange interactions, if any, are close in magnitude and are mutually compensating. As a result, the dependence $\mu_{\text{eff}}(T)$ for [Cu(SQ)$_2$-NIT-*m*Py]·C_6H_6 in the range 100−300 K is an almost straight line parallel to the abscissa, and the asymptotic value of the magnetic moment at room temperature is close to the theoretical value (3.46 μ_B) for four almost non-interacting spins with $S = {}^1\!/_2$ and $g = 2$. In [Cu(SQ)$_2$Py]·C_7H_8 and [Cu(SQ)$_2$Py]·Et_2O, where the environment of Cu is completed by pyridine, the ferromagnetic channel of exchange interaction is dominant. Treatment of the experimental dependence $\mu_{\text{eff}}(T)$ for [Cu(SQ)$_2$Py]·C_7H_8 using the above-mentioned spin Hamiltonian gave the following optimal values of exchange parameters: $J = 222$ cm^{-1} and $J_1 = -76$ cm^{-1} (the theoretical curve in Figure 3 is shown as a solid line). Moreover, ferromagnetic exchange also prevails in solid Cu(SQ)$_2$DABCO (Figure 3), although the donor N atoms are separated by very long distances ($d_{\text{Cu-N}} = 2.69(1)$ Å) from the planar matrix of Cu(SQ)$_2$. To explain these experimental facts, we had to perform a quantum chemical study.

---

[19] Abakumov, G. A.; Krashilina, A. V.; Cherkasov, V. K.; Eremenko, I. L.; Nefedov, S. E. *Russ. Chem. Bull.* **2001**, *50*, 2193−2199.

DFT Calculations. For the three-center system shown in Chart 2, the exchange coupling parameters J and J_1 were calculated using the "broken symmetry" (BS) approach.[20] For $Cu(SQ)_2$, $[Cu(SQ)_2Py]{\cdot}C_7H_8$, $[Cu(SQ)_2Py]{\cdot}Et_2O$, and $Cu(SQ)_2$-DABCO molecules, each containing three exchange-coupled paramagnetic centers with spin $^1/_2$ for each center, exchange interactions were described using the spin Hamiltonian:

$$\hat{H} = -2J\,\hat{s}_{Cu}(\hat{s}_{SQ1} + \hat{s}_{SQ2}) - 2J_1\,\hat{s}_{SQ1}\,\hat{s}_{SQ2} \qquad (1)$$

The exchange coupling parameters of Hamiltonian (1) were calculated from the mean energies of the BS solutions corresponding to different spin density distributions within the complex. The generalized spin projection method suggested by Yamaguchi et al.[21] yields

$$J = -\frac{E_{\alpha\alpha\alpha} - E_{\alpha\beta\alpha}}{\langle S^2\rangle_{\alpha\alpha\alpha} - \langle S^2\rangle_{\alpha\beta\alpha}};\qquad J_1 = -\frac{E_{\alpha\alpha\alpha} - 2E_{\alpha\alpha\beta} + E_{\alpha\beta\alpha}}{\langle S^2\rangle_{\alpha\alpha\alpha} - 2\langle S^2\rangle_{\alpha\alpha\beta} + \langle S^2\rangle_{\alpha\beta\alpha}}$$

The energy difference between the states with different multiplicities for three-spin systems described by spin Hamiltonian (1) is

$$\Delta E_1 = E_1(S = {}^1/_2) - E(S = {}^3/_2) = 2J_1 + J$$

$$\Delta E_2 = E_2(S = {}^1/_2) - E(S = {}^3/_2) = 3J$$

Here, $E_1(S = {}^1/_2)$ and $E_2(S = {}^1/_2)$ are eigenvalues of Hamiltonian (1), corresponding to $S = {}^1/_2$, and $E(S = {}^3/_2)$ is the energy of the high-spin state of the complex.

For the four-spin system of $[Cu(SQ)_2NIT\text{-}m\mathrm{Py}]{\cdot}C_6H_6$, the spin Hamiltonian is of the form

$$\hat{H} = -2J\,\hat{s}_{Cu}(\hat{s}_{SQ1} + \hat{s}_{SQ2}) - 2J_1\,\hat{s}_{SQ1}\,\hat{s}_{SQ2} - 2J_1\,\hat{s}_{Cu}\,\hat{s}_{R} \qquad (2)$$

and the exchange coupling parameters may be sought as

$$J = \frac{E_{\alpha\beta\alpha\alpha} - E_{\alpha\alpha\alpha\beta}}{2 - \langle S^2\rangle_{\alpha\beta\alpha\alpha} + \langle S^2\rangle_{\alpha\alpha\alpha\beta}}$$

$$J_1 = -\frac{2E_{\alpha\alpha\alpha\alpha} - 2E_{\alpha\alpha\beta\alpha} + E_{\alpha\beta\alpha\alpha} - E_{\alpha\alpha\alpha\beta}}{4 - 2\langle S^2\rangle_{\alpha\alpha\alpha\alpha} + 2\langle S^2\rangle_{\alpha\alpha\beta\alpha} - \langle S^2\rangle_{\alpha\beta\alpha\alpha} + \langle S^2\rangle_{\alpha\alpha\alpha\beta}}$$

$$J_2 = \frac{E_{\alpha\alpha\alpha\alpha} - E_{\alpha\alpha\alpha\beta}}{2 - \langle S^2\rangle_{\alpha\alpha\alpha\alpha} + \langle S^2\rangle_{\alpha\alpha\alpha\beta}}$$

For describing the molecular orbitals of $Cu(SQ)_2$, the Cu atom was placed at the center of the coordinate system, the z-axis was chosen running along the normal to the chelate plane, the x-axis was chosen running along the "long" axis of the complex through the middle of the C−C bonds of the carbon atoms bonded to the O atoms, and the y-axis was chosen running along the "long" axis of the complex, as shown in Chart 4.

Chart 4

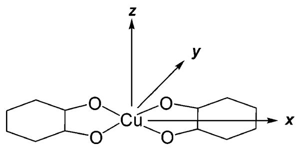

Figure 4 presents a view of the magnetic orbitals of $Cu(SQ)_2$ according to the data of UB3LYP calculation for the ααα state corresponding to the maximum spin of the molecule. The energy scheme of the mutual arrangement of these orbitals is shown in Figure 5. Orbitals **1** and **2** correspond to the symmetric and antisymmetric combinations of the singly occupied orbitals of the two semiquinonate radical anions.[22] Symmetry analysis indicates that only orbital **1** can interact with the Cu $3d_{xz}$ orbital, and, according to calculations, it has a contribution of ∼2% from the Cu atom. Increased splitting between the symmetric and antisymmetric magnetic orbitals leads to increased efficiency of antiferromagnetic exchange coupling.[23] In the case of $Cu(SQ)_2$, this splitting is caused by the interaction of magnetic orbital **1** with the central Cu atom. Since this is an antibonding interaction, it leads to increased energy of orbital **1** compared to the energy of orbital **2** (Figure 5). *The superexchange channel via the Cu atom dominates in the observed antiferromagnetic interaction of ligands*. Therefore, the efficiency of this pathway may depend on minor distortions of the coordination polyhedron, leading to deviation of the Cu atom or atoms of one of the SQ ligands from the xy plane and changing the distances between the paramagnetic centers within the limits of the xy plane (Chart 4).

Magnetic orbital **3** is centered on the Cu atom and dominates in the $3d_{x^2-y^2}$ orbitals. The pronounced contribution from the p_x and p_y orbitals of the O atoms of the semiquinone fragments to orbital **3** leads to a *strong direct ferromagnetic exchange in the Cu−SQ channel*. The form of the magnetic orbitals does not radically change for the whole series of complexes under discussion. Figure 6 shows spin density distribution for the broken symmetry states.

Table 2 summarizes the results of quantum chemical calculations of exchange coupling parameters. In the given series of compounds, the efficiency of the direct ferromagnetic interaction channel J (values not included in parentheses) changes only slightly from complex to complex. At the same time, changes in the coordination polyhedron strongly affect the exchange coupling parameter J_1 between ligands. This effect is so drastic that it changes the multiplicity of the ground state of the complex. The last column of Table 2 shows that the next energy level of the system is much higher in energy and is therefore excluded from further analysis.

Since changes in the coordination environment can be different and mutually enhancing, we attempted to analyze them separately. For this we performed a series of model calculations. Figure 1b,b′ and c,c′ shows the distortions of the coordination

---

[20] (a) Daul, C. A.; Ciofini, I.; Bencini, A. In *Reviews of Modern Quantum Chemistry. Part II;* Sen, K. D., Ed.; World Scientific, Singapore, 2002; pp 1247−1294. (b) Noodleman, L.; Peng, C. Y.; Case, D. A.; Mouesca, J. M. *Coord. Chem. Rev.* **1995**, *144*, 199−244. (c) Noodleman, L.; Norman, J. G., Jr. *J. Chem. Phys.* **1979**, *70*, 4903−4906.

[21] (a) Shoji, M.; Koizumi, K.; Kitagawa, Y.; Kawakami, T.; Yamanaka, S.; Okumura, M.; Yamaguchi, K. *Chem. Phys. Lett.* **2006**, *432*, 343−347. (b) Soda, T.; Kitagawa, Y.; Onishi, T.; Takano, Y.; Shigeta, Y.; Nagao, H.; Yoshioka, Y.; Yamaguchi, K. *Chem. Phys. Lett.* **2000**, *319*, 223−230. (c) Yamaguchi, K.; Jensen, F.; Dorigo, A.; Houk, K. N. *Chem. Phys. Lett.* **1988**, *149*, 537−542.

[22] (a) Herebian, D.; Wieghardt, K. E.; Neese, F. *J. Am. Chem. Soc.* **2003**, *125*, 10997−11005. (b) Bencini, A.; Carbonera, C.; Totti, F. *Chem. Eur. J.* **2004**, *10*, 1472−1480.

[23] Hay, P. J.; Thibeaut, J. C.; Hoffmann, R. *J. Am. Chem. Soc.* **1975**, *97*, 4884−4899.

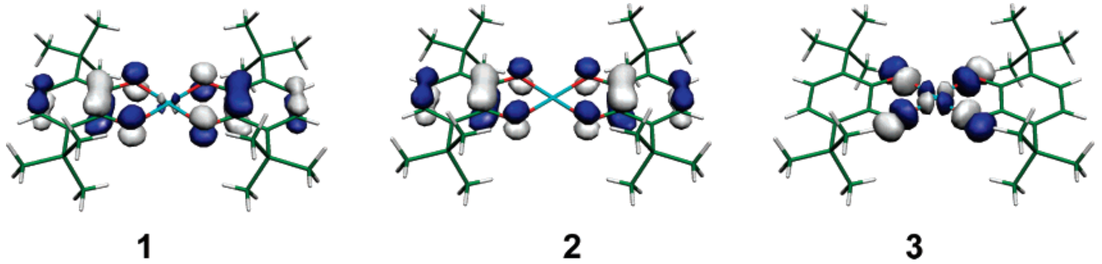

Figure 4. Magnetic orbitals of $Cu(SQ)_2$.

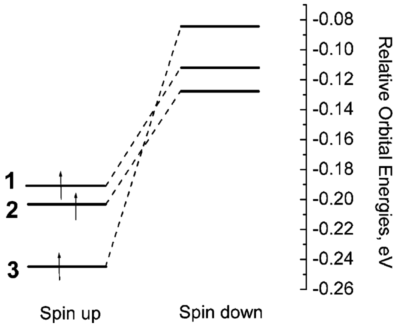

Figure 5. Energy scheme of magnetic orbitals **1**, **2**, and **3** for the high-spin state of $Cu(SQ)_2$.

unit in $[Cu(SQ)_2Py]{\cdot}C_7H_8$ and $[Cu(SQ)_2NIT\text{-}m\text{Py}]{\cdot}C_6H_6$, respectively, which prompted us to perform a series of calculations to model the effects of the Cu atom deviating from the plane and the effects of the plane of one of the SQ ligands rotated around the y-axis (in the latter case, the copper atom stays at the origin). In both cases, for the initial geometry we used X-ray diffraction data for $Cu(SQ)_2$. These calculations indicated that the nonplanar structure of the CuO_4 coordination unit does not violate the orthogonal structure of the copper-centered orbital **3** relative to magnetic orbitals **1** and **2** (Figure 4) localized on the ligands and does not lead to significant changes in the exchange coupling parameter J. Both the axial shift of the Cu atom to a distance $\Delta z \approx 0.1-0.5$ Å from the plane of the CuO_4 unit (Figure 7) and rotation of the plane of one of the SQ ligands within the angle $0 < \varphi < 15°$ around the y-axis (Figure 8) do not change the efficiency of the Cu−SQ exchange interaction. However, even a minor axial shift of the copper atom from the chelate plane decreases the contribution of Cu $3d_{xz}$ to magnetic orbitals **1** and **2**, which, in turn, has a pronounced effect on the efficiency of the antiferromagnetic exchange coupling channel between ligands. The drastic decrease in the value of J_1 can, in principle, change the multiplicity of the ground state of the complex (Figure 7, red line). However, evolution of J_1 is extremely small within the limits of the values of φ under study (Figure 8).

As mentioned above, the additional ligands appearing in the coordination sphere lead to elongated Cu−O distances. Thus, while in $Cu(SQ)_2$ the Cu−O distances are 1.910 ± 0.005 Å at 240 and 110 K (i.e., variation of temperature has a very insignificant effect in this case), in other compounds the same distances are 1.941 ± 0.007 Å in $[Cu(SQ)_2NIT\text{-}m\text{Py}]{\cdot}C_6H_6$, 1.943 ± 0.004 Å in $[Cu(SQ)_2Py]{\cdot}C_7H_8$, 1.938 ± 0.010 Å in $[Cu(SQ)_2Py]{\cdot}Et_2O$, and 1.956 ± 0.004 Å in $Cu(SQ)_2DABCO$. Thus, the Cu−O distances increase by hundredths of an angstrom from $Cu(SQ)_2$ to mixed-ligand complexes. Note, however, that elongation of the distance between the SQ ligands even by this magnitude along the x axis in the xy plane (Chart 4) leads to a significant decrease in $|J_1|$ relative to J (Figure 9), which can also dramatically change the ratio between the ferro- and antiferromagnetic exchange energies.

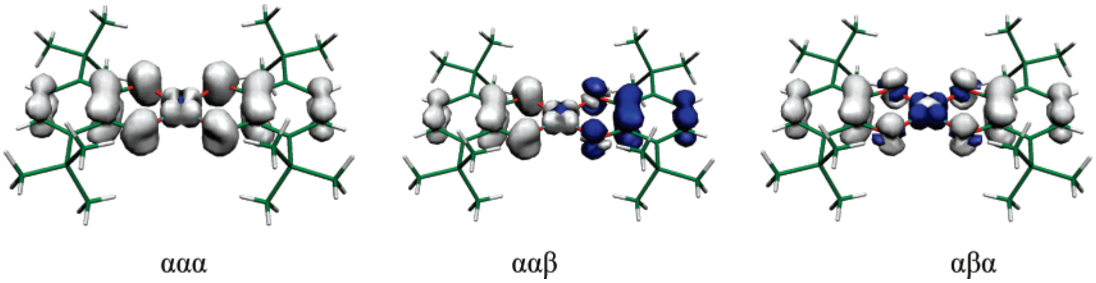

Figure 6. Spin density distribution for the broken symmetry states of $Cu(SQ)_2$.

Table 2. Calculated Exchange Coupling Parameters and Energy Differences between Multiplets (cm^{-1}) (the Values for Model Systems are Given in Parentheses)

no.	complex	J	J_1	$E_1(^1/_2) - E(^3/_2)$	$E_2(^1/_2) - E(^3/_2)$
I	$Cu(SQ)_2$	+300	−327	−354	900
II	$[Cu(SQ)_2NIT\text{-}m\text{Py}]{\cdot}C_6H_6$	+331 (+282)	−125 (−261)	81^a (−240)	993^a (846)
III	$[Cu(SQ)_2Py]{\cdot}C_7H_8$	+320 (+274)	−120 (−250)	80 (−226)	962 (750)
IV	$[Cu(SQ)_2Py]{\cdot}Et_2O^b$	+331 (+271)	−118 (−262)	95 (−253)	997 (786)
V	$[Cu(SQ)_2Py]{\cdot}Et_2O^b$	+351 (+322)	−222 (−314)	−93 (−306)	1055 (942)
VI	$Cu(SQ)_2DABCO$	+275 (+262)	−68 (−232)	139 (−202)	811 (696)

[a] For $[Cu(SQ)_2NIT\text{-}m\text{Py}]{\cdot}C_6H_6$, the given energy differences correspond to the states of the three-spin exchange cluster with the given exchange coupling parameters J and J_1 and do not allow for interaction with the spin of the radical, $J_2 \approx +1$ cm^{-1}. [b] Calculated data for each of the two $[Cu(SQ)_2Py]{\cdot}Et_2O$ independent molecules.

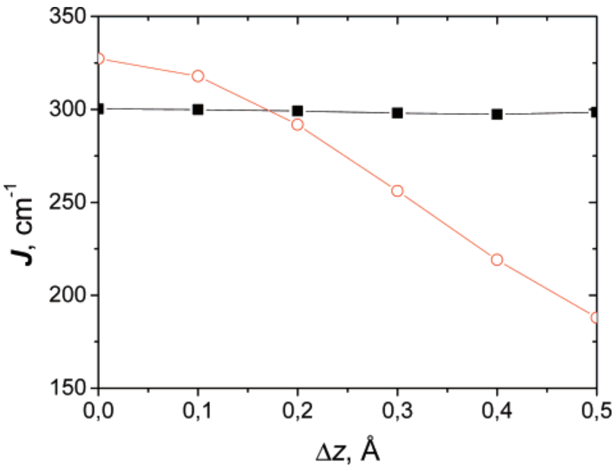

Figure 7. Effects of the axial displacement (Δ*z*) of the Cu atom from the plane of the CuO_4 coordination unit on the values of *J* (black, ■) and $|J_1|$ (red, ○) in the $Cu(SQ)_2$ matrix.

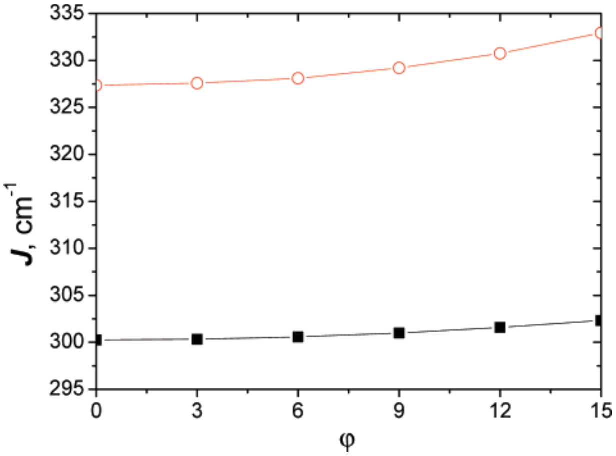

Figure 8. Effects of rotation of the plane of one of the SQ ligands around the *y*-axis on *J* (black, ■) and $|J_1|$ (red, ○) in the $Cu(SQ)_2$ matrix.

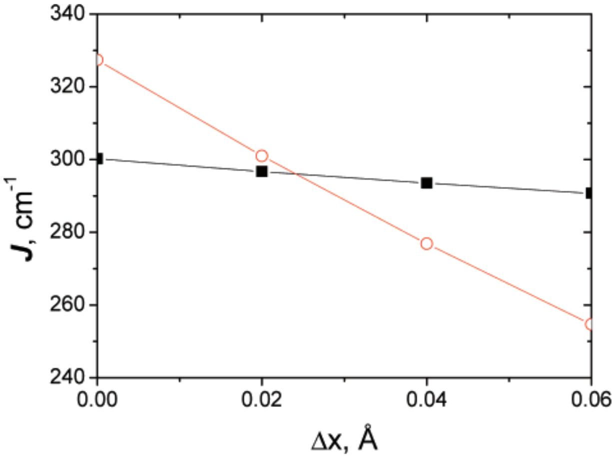

Figure 9. Effects of separation of the SQ ligands on *J* (black, ■) and $|J_1|$ (red, ○) in the $Cu(SQ)_2$ matrix.

Table 3. Calculated Exchange Coupling Parameters for Different Cu−N Distances

$Cu(SQ)_2Py$			$Cu(SQ)_2DABCO$		
d_{CuN}, Å	J, cm^{-1}	J_1, cm^{-1}	d_{CuN}, Å	J, cm^{-1}	J_1, cm^{-1}
2.25	+346	−171	2.6	+325	−85
2.30	+340	−185	2.7	+323	−105
2.35	+335	−196	2.8	+321	−126
∞[a]	+300	−327	∞[a]	+300	−327

[a] The values of J and J_1 for infinitely long distances d_{CuN} actually correspond to the parameters for $Cu(SQ)_2$.

In every case, one of the factors or their combination may appear to be critical. However, it is important to consider the information provided by calculations for $\{Cu(SQ)_2\}$ fragments actually found in the mixed-ligand complexes under study (nos. II−VI, Table 2). To generate these fragments before calculations, the extra ligand (NIT-*m*Py, Py, or DABCO) was removed from the coordination sphere; for the remaining $\{Cu(SQ)_2\}$ fragment, we used the geometry found in the X-ray experiment. The exchange coupling parameters and the energy differences between the multiplets obtained in this way and given in parentheses in Table 2 are very important. In the column that gives J_1, the values in parentheses are much larger than those outside the parentheses and are comparable to the values of ferromagnetic exchange J. If we take into account that $\Delta E_1 = 2J_1 + J$, then the high-spin ground state is not observed for any of the $\{Cu(SQ)_2\}$ model fragments under study. Consequently, there is another strong effect on the ratio between J and J_1. It appeared that this effect is related to redistribution of the odd-electron density in the complex compared to the distribution in free $Cu(SQ)_2$. This redistribution, in turn, depends significantly on the nature and orientation of the extra ligand (NIT-*m*Py, Py, or DABCO in our case). Thus, the results of our calculations directly point to the importance of an extra ligand being available in the coordination sphere because the effects of the distorted $\{Cu(SQ)_2\}$ chelate matrix caused by the extra ligand do not change the ground spin state of the matrix. This suggested to us that the $Cu(SQ)_2$ matrix plays a special role: when coordinating the extra ligand, it automatically acts as an *environment sensor* operated by the variation of the ferro- to antiferromagnetic exchange ratio in the $Cu(SQ)_2$ fragment.

To illustrate the role of the extra ligand, let us first address Table 3. It gives the results of a series of calculations for $Cu(SQ)_2Py$ and $Cu(SQ)_2DABCO$ model complexes in which the distance between the N atom of the extra ligand and the Cu atom of the undistorted $Cu(SQ)_2$ matrix was varied. The average value of d_{CuN} was chosen in accordance with the experimental values for both $Cu(SQ)_2Py$ and $Cu(SQ)_2DABCO$: 2.305(7) Å for $[Cu(SQ)_2Py]\cdot C_7H_8$ and 2.69(1) Å for $Cu(SQ)_2DABCO$. As can be seen from Table 3, the approach of the nitrogen donor atom of the ligand to the $Cu(SQ)_2$ matrix leads to slightly increased values of J and dramatically decreased values of $|J_1|$. This indicates that the approach of the nitrogen-containing ligand to the $Cu(SQ)_2$ matrix *mainly affects the antiferromagnetic exchange channel.* This is a nontrivial result because this exchange channel is mainly related to magnetic orbitals **1** and **2** of the semiquinonate ligands (Figure 4). The Cu $3d_{xz}$ orbital, which must not be very sensitive to variation of the Cu−N distance, makes a small contribution (∼2%) to orbital **1**.

The relationship between the exchange channels J and J_1 is substantially affected by the HOMO of the extra ligand (Py or DABCO) (Figures 10c and 11b) mixed with both the doubly occupied orbital of $Cu(SQ)_2$ (Cu d_{z^2} orbital) and magnetic orbital **2** (a combination of the singly occupied orbitals of SQ). This results in redistribution of odd-electron density and in its partial *delocalization* to the N atom of the extra ligand. The strength of this effect depends not only on the distance between the N atom and the Cu atom of the bischelate but also on the

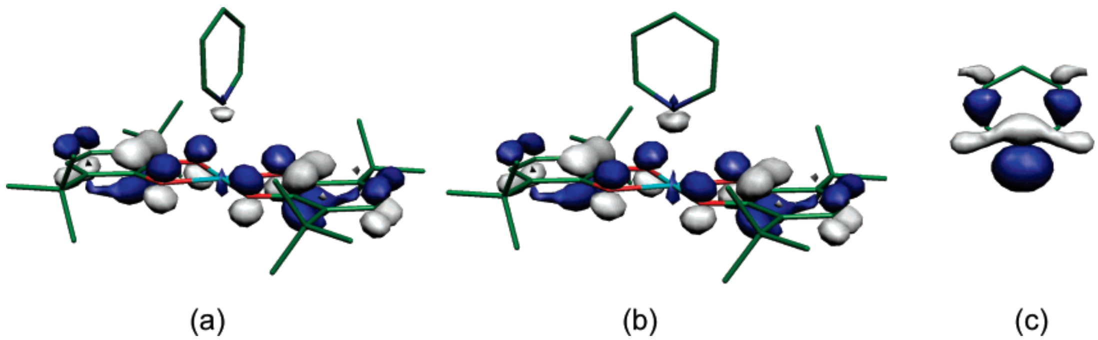

Figure 10. Transformation of magnetic orbital **2** for the arrangement of the heterocycle in the *yz* (a) and *xz* (b) planes. The HOMO of pyridine is also shown (c). Hydrogen atoms are omitted for clarity.

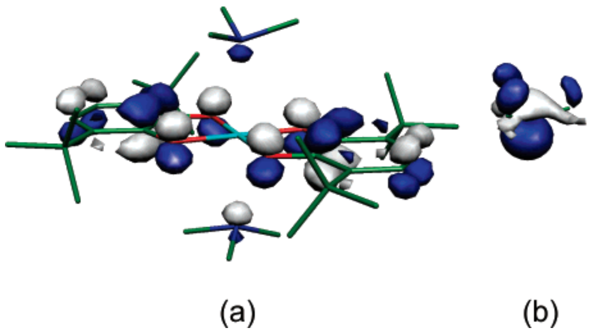

Figure 11. Transformation of magnetic orbital **2** for two trimethylamine molecules (a). The HOMO of trimethylamine that models DABCO is also shown (b). Hydrogen atoms are omitted for clarity.

orientation of the ligand relative to the $Cu(SQ)_2$ matrix. Figure 10 shows transformation of magnetic orbital **2** (Figure 4) for the Py ligand coordinated at a distance $d_{CuN} = 2.30$ Å and having two different orientations. In one instance, the pyridine ring lies in the *yz* plane (Figure 10a), as it does in real $Cu(SQ)_2Py$ structures; in the other, it lies in the *xz* plane (Figure 10b). It can be seen that, in case "b", the magnetic orbital is much more delocalized to the N atom of pyridine. Therefore, this orientation is more favorable for mixing the orbitals of the complex and diamagnetic ligand, which affects the efficiency of the antiferromagnetic channel of exchange interaction: $J_1 = -185$ cm^{-1} for the pyridine ring lying in the *yz* plane (Table 3) and $J_1 = -116$ cm^{-1} for the ring in the *xz* plane. The orientation of the heterocycle has a less pronounced effect on ferromagnetic exchange: $J = +340$ cm^{-1} (*yz*) and $J = +357$ cm^{-1} (*xz*).

In view of the given mixing of orbitals, we can understand the effect of the nature of the extra ligand on the efficiency of the exchange channels. Thus, although the DABCO complex has much longer distances d_{CuN}, the presence of DABCO in the coordination sphere of the complex has a dramatic effect on the odd-electron density redistribution, because the orbital with a donor electron pair in DABCO is longer than the similar orbital in Py. In this case, the doubly occupied orbital of $Cu(SQ)_2DABCO$, which corresponds to a symmetric combination of the HOMOs of two DABCO molecules modeled by two trimethylamine molecules, has a significant admixture of d_{z^2} Cu: the antisymmetric combination of these orbitals is admixed with magnetic orbital **2**, giving a significant contribution to the resulting magnetic orbital of the complex (Figure 11a). This substantial delocalization of the magnetic orbital to the N atoms of DABCO molecules is responsible for the drastic change in the exchange energy in channel J_1 in $Cu(SQ)_2DABCO$.

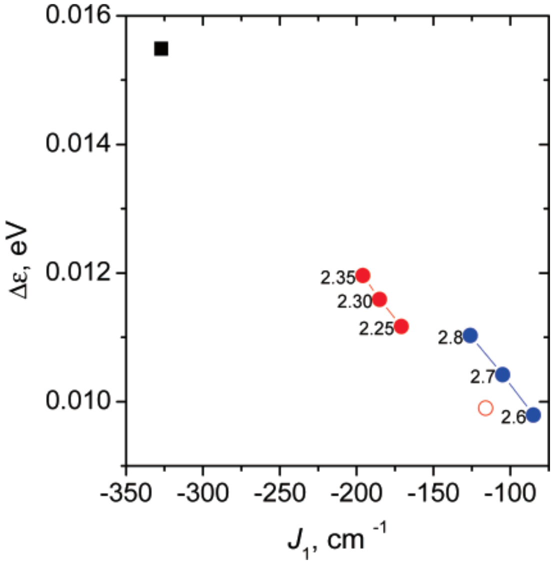

Figure 12. Correlation between the orbital energy difference and the calculated exchange coupling parameters J_1 for $Cu(SQ)_2$ (black, ■), $Cu(SQ)_2Py$ (red, ● for Py in the *yz* plane ○ for Py in the *xz* plane), and $Cu(SQ)_2DABCO$ (blue, ●) model complexes. The labels give the distances d_{CuN} (Å) for the series of $Cu(SQ)_2Py$ and $Cu(SQ)_2DABCO$ model complexes.

The interaction of magnetic orbital **2** of the $Cu(SQ)_2$ complex with the orbitals of Py or DABCO is antibonding (Figures 10 and 11), while magnetic orbital **1** is not involved in this interaction. This leads to decreased splitting between magnetic orbitals **1** and **2** and hence to lower efficiency of the antiferromagnetic channel of the exchange interaction (Figure 12). The data in Figure 12 reflect the most important magnetostructural correlations inherent in the nature of the $Cu(SQ)_2$ sensor under discussion.

Conclusions

As a result of our study, initially aimed at investigating the possibility of synthesizing multispin complexes of Cu(II) with *o*-semiquinonate and nitronyl nitroxide ligands in the coordination sphere, we have isolated the first compound of a new type, $[Cu(SQ)_2NIT\text{-}m\text{Py}]\cdot C_6H_6$, and a series of model complexes of $Cu(SQ)_2$ with diamagnetic Py and DABCO and defined their structure. More importantly, analysis of the magnetic properties of this series of heterospin complexes in a special quantum chemical study provided an explanation for the unusual effect of the suppressed intramolecular channel of antiferromagnetic exchange in $Cu(SQ)_2$, resulting from coordination of extra ligands. The energy of the exchange interaction between the odd electrons of the SQ ligands was found to be extremely sensitive to the occurrence of an extra ligand in the coordination sphere of Cu(II) and to the nature of this ligand. Our results actually indicate that bis(3,6-di-*tert*-butyl-*o*-benzosemiquinonato)copper(II) behaves as a polyfunctional molecular sensor for the first coordination sphere of the central atom. The Cu(II) is not confined to the role of the driving force, incorporating an extra ligand in its coordination sphere. The electronic structure of Cu(II) provides a specific combination of the intramolecular channels of ferro- and antiferromagnetic exchange with two SQ ligands. However, after an extra ligand has appeared in the vicinity of the $Cu(SQ)_2$ matrix, the odd-electron density undergoes redistribution in the antiferromagnetic exchange channel, caused by the magnetic orbitals of the SQ ligands. Quantum chemical analysis of exchange interactions has completely confirmed that the indirect exchange parameter J_1 is highly sensitive to variation of the geometrical characteristics of the $\{SQ^{-\bullet}-Cu^{2+}-{}^{\bullet}SQ^{-}\}$ exchange cluster and to the incorporation of an extra ligand in the coordination sphere.

Thus, the results of our study show that $Cu(SQ)_2$ is an unusual type of molecular sensor operated by variation of the ferro- to antiferromagnetic exchange ratio.

Acknowledgment. This research was supported by RFBR (grants 04-03-32409, 06-03-32157, 06-03-08004, 05-03-32305, and 06-03-32742), CRDF (grant RUE1-2839-NO-06), the President of Russia (grants NSh 4947.2006.3, MK-1739.2005.3, MK-4362.2006.3, and MK-10264.2006.3), Russian Academy of Sciences, and Siberian Branch, Russian Academy of Sciences. We gratefully acknowledge G. K. Boreskov Institute of Catalysis for providing access to the computational facilities.

Supporting Information Available: CIF files for all complexes; complete ref 13. This material is available free of charge via the Internet at http://pubs.acs.org.

JA072463B